Hettiwatte, S.N., Wang, Z.D. and Crossley, P.A. (2001) Transformer modelling for studying the propagation of partial discharge pulses. In: UPEC 2001, 36th Universities' Power Engineering Conference, 12 - 14 September, Swansea.

TRANSFORMER MODELLING FOR STUDYING THE PROPAGATION OF PARTIAL DISCHARGE PULSES

S. N. Hettiwatte, Z. D. Wang and P. A. Crossley

UMIST, UK

ABSTRACT

A computer model developed for studying the propagation of partial discharge (PD) pulses in a continuous disc type 6.6 kV transformer winding is described in the paper. The winding model takes the turn as the basis for the analysis and uses multi-conductor transmission line theory to obtain a system of equations to calculate the voltage and current along the winding. Capacitance, inductance, resistance and conductance are calculated as distributed parameters for the winding model. Transfer functions that can be used to study the effect on the PD current as the monitoring point moves from the location of the PD to the line-end and the neutral-end are calculated. The transfer functions represent the frequency response of the signals measured at the line and neutral-end terminals for a PD pulse represented by a Dirac delta function at the point of discharge. The zeros of the transfer functions convey information about the position of the discharge and hence can be used for its location.

INTRODUCTION

A partial discharge (PD) is defined as a localised electrical discharge that only partially bridges the insulation between conductors and which may, or may not, occur adjacent to a conductor [1]. Partial discharges are steep fronted pulses having duration from fractions of nano-seconds (ns) to a few microseconds (μs). The frequency spectra of such PD pulses can extend beyond 1 GHz. Ideally, to study all types of PD propagation through a transformer winding, one has to accurately model the winding from a few hundred kHz to a few GHz. Such an ultra wide band circuit is difficult to simulate. Hence, a compromise solution is required and this involves the design of a model suitable for frequencies from a few hundred kHz to a few tens of MHz. Such a model is suitable for representing the effect on a PD pulse (duration 100 ns ~ 10 μs) of propagating along the transformer winding.

Previous research [2] has shown that a lumped element representation of each disc in a transformer winding is valid for frequencies up to a few hundred kHz. However, electromagnetic (EM) wave propagation in the winding at higher frequencies requires more resolution. Hence, each turn of the winding is taken as a lumped element and multi-conductor transmission line (MTL) theory is then used to represent the complete winding [3].

The capacitance, inductance, resistance and conductance values are calculated per turn as the inputs. These parameter values consist of matrices with dimensions equal to the number of turns in the winding. Transfer functions that describe the effect on the PD current in moving from the source of the discharge to the line-end and the neutral-end of the winding are used in the PD propagation studies [2]. A simulation program developed in Matlab® Version 5.3 (R11) was used to calculate these transfer functions. The simulation results show that the zeros in the transfer functions contain information about the location of discharge [2].

THE MULTI-CONDUCTOR WINDING MODEL

MTL theory is applicable to a set of conductors in an EM field provided that the wave propagation is transverse electromagnetic (TEM) [4]. When the wavelength of propagation (λ) is very large compared with the cross-sectional dimensions of conductors, as is the case in this study, the wave propagation is usually by TEM mode and hence MTL theory can be applied. Figure 1 shows the representation of a winding using a MTL model.

The voltage (V) and the current (I) distributions in such a system can be derived from the wave equations (1) and (2), where [Z] and [Y] are impedance and admittance matrices of the line respectively, and $[P]^2 = [Z][Y]$, $[P_t]^2 = [Y][Z]$.

$$\frac{d^2V}{dx^2} = [Z][Y]V = [P^2]V \tag{1}$$

$$\frac{d^2I}{dx^2} = [Y][Z]I = [P_t^{\,2}]I \tag{2}$$

Equation (1) and (2) can be solved to give

$$V_x = V_1 e^{(-[P]x)} + V_2 e^{([P]x)} \tag{3}$$

$$I_x = Y_O(V_1 e^{(-[P]x)} - V_2 e^{([P]\ x)}) \tag{4}$$

where V_1 and V_2 are constants to be determined by the terminal conditions, $[Y_O] = [Z]^{-1}[P] = [Y][P]^{-1}$ is the characteristic admittance of the network and x is the distance measured from the sending end of the transmission lines.

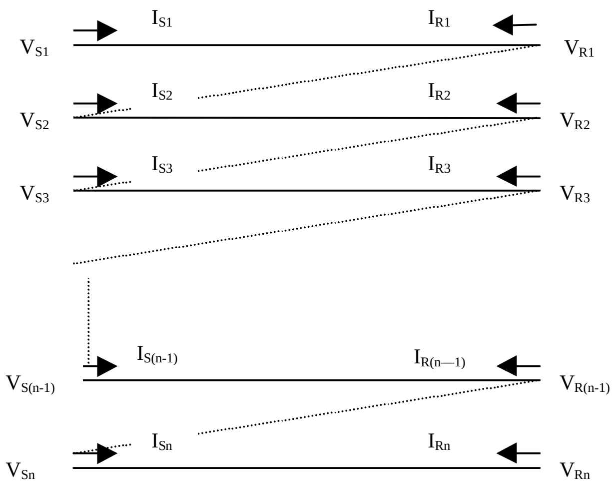

Figure 1 Multi-conductor transmission line model

If terminal conditions are applied to Equation (3) and (4) for x=0 and x=l, where l is the average length of a transmission line, it will lead to

$$V_S = V_1 + V_2 \tag{5a}$$

$$I_S = Y_O(V_1 - V_2) \tag{5b}$$

$$V_R = V_1 e^{-[P]l} + V_2 e^{[P]l} \tag{5c}$$

$$I_R = Y_O(V_1 e^{-[P]l} - V_2 e^{[P]l}) \tag{5d}$$

where sending end quantities are denoted by the subscript '$_S$' and the receiving end quantities by '$_R$'. Equation (5a), (5b), (5c) and (5d) can be used to express I_S and I_R in terms of V_S and V_R.

$$\begin{pmatrix} I_S \\ I_R \end{pmatrix} = Y_O \begin{pmatrix} \coth([P]l) & \cos ec([P]l) \\ \cos ec([P]l) & \coth([P]l) \end{pmatrix} \begin{pmatrix} V_S \\ V_R \end{pmatrix} \tag{6}$$

Equation (6) has exponentials of matrix [P], which can be calculated by diagonalising [P]. If [P] has eigen vectors [Q] and eigen values [γ], [P] can be written as

$$[P] = [Q][g][Q]^{-1} \tag{7}$$

From Equations (6) and (7) it is possible to derive

$$\begin{pmatrix} I_S \\ I_R \end{pmatrix} = \begin{pmatrix} [A] & -[B] \\ -[B] & [A] \end{pmatrix} \begin{pmatrix} V_S \\ V_R \end{pmatrix} \tag{8}$$

where $[A] = [Y][Q][\gamma]^{-1}\coth([\gamma]l)[Q]^{-1}$ and $[B] = [Y][Q][\gamma]^{-1}\text{cosech}([\gamma]l)[Q]^{-1}$ are $n \times n$ matrices, and n is the number of conductors in the model. I_S, I_R, V_S and V_R are vector quantities representing the values in Figure 1. The transmission line model in Figure 1 has terminal conditions:

$$I_R(i) = -I_S(i+1) \quad \text{for } i = 1 \text{ to } n-1 \tag{9}$$

$$V_R(i) = V_S(i+1) \quad \text{for } i = 1 \text{ to } n-1 \tag{10}$$

With this set of terminal conditions applied to Equation (8), it is possible to do two types of reduction [3]:

(i) With Equation (9), adding rows of the matrix in Equation (8), all the currents can be discarded except $I_S(1)$ and $I_R(n)$.

(ii) With Equation (10), adding columns of the matrix in Equation (8), all receiving end voltages, except $V_R(n)$ can be discarded.

With these reductions Equation (8) becomes

$$\begin{pmatrix} I_S(1) \\ 0 \\ . \\ . \\ . \\ . \\ . \\ . \\ 0 \\ I_R(n) \end{pmatrix} = \begin{pmatrix} \\ \\ \\ \\ [Y] \\ \\ \\ \\ \end{pmatrix} \begin{pmatrix} V_S(1) \\ V_S(2) \\ . \\ . \\ . \\ . \\ . \\ . \\ V_S(n) \\ V_R(n) \end{pmatrix} \tag{11}$$

where [Y] is a $(n+1) \times (n+1)$ matrix.

PD injection

If a PD current pulse I_{PD} is injected into the k^{th} turn of the winding, Equation (9) is modified when i = k-1:

$$I_R(k-1) + I_S(k) = I_{PD} \tag{12}$$

All other rows in Equation (9) remain unchanged. If this change is incorporated into Equation (11), only the current vector in row k is modified. The new equation is

$$\begin{pmatrix} I_S(1) \\ 0 \\ . \\ 0 \\ I_{PD} \\ 0 \\ . \\ . \\ 0 \\ I_R(n) \end{pmatrix} = \begin{pmatrix} \\ \\ \\ \\ [Y] \\ \\ \\ \\ \end{pmatrix} \begin{pmatrix} V_S(1) \\ V_S(2) \\ . \\ . \\ V_S(k) \\ . \\ . \\ . \\ V_S(n) \\ V_R(n) \end{pmatrix} \tag{13}$$

If matrix [Y] is inverted and re-arranged, it is possible to get Equation (14).

Hence, if the line-end voltages, the neutral-end currents and the PD current are known all other voltages and currents can be calculated.

$$\begin{pmatrix} I_S(1)\\ V_S(2)\\ V_S(3)\\ .\\ V_S(k)\\ .\\ .\\ .\\ V_S(n)\\ V_R(n)\end{pmatrix} = \begin{pmatrix} & & \\ & [T] & \\ & & \end{pmatrix} \begin{pmatrix} V_S(1)\\ 0\\ .\\ 0\\ I_{PD}\\ 0\\ .\\ .\\ 0\\ I_R(n)\end{pmatrix} \quad (14)$$

If the bushing capacitance C_B represents a boundary condition at the line-end, then

$$I_S(1) = -jwC_B V_S(1) \quad (15)$$

If the neutral-end is at earth potential, the boundary condition at the neutral-end will be

$$V_R(n) = 0 \quad (16)$$

With these boundary conditions, the transfer function from the PD source current to the line-end current (TF_L) is

$$\frac{I_S(1)}{I_{PD}} = \frac{T(1,k)T(N,N) - T(N,k)T(1,N)}{T(N,N) + \frac{1}{j2pfC_B}\left(T(1,1)T(N,N) - T(N,1)T(1,N)\right)} \quad (17)$$

where N=n+1. Similarly, the transfer function from the PD source current to the neutral-end current (TF_N) is

$$\frac{I_R(n)}{I_{PD}} = \frac{T(N,1)TF_L - j2pfC_B T(N,k)}{T(N,N)\, j2pfC_B} \quad (18)$$

CALCULATION OF ELECTRICAL PARAMETERS

The physical dimensions of a transformer winding and the permittivity of the insulation are used to construct this 22-section × 13-turn, continuous type winding. The impedance and admittance matrices in Equation (1) and (2) are calculated using:

$$[Z] = R_S[I_n] + j2pf[L] \quad (19)$$

$$[Y] = [G] + j2pf[C] \quad (20)$$

where R_S = resistance, [L] = inductance matrix, [G] = conductance matrix, [C] = capacitance matrix, [I_n] = unit matrix and f is the frequency.

Capacitance

Capacitance and inductance are the most important parameters since they play a major role in the accuracy of this model. The capacitive elements are the most straightforward to evaluate since they only involve calculations based on geometry and permittivity of insulation. In capacitance calculations there are three components to be considered: inter-turn capacitance (CIT), inter-section capacitance (CID) and capacitance to the low voltage winding (CLV). CIT is calculated assuming two adjacent turns of the winding form a parallel plate capacitor. This assumption is also used in the calculation of CID. Greater accuracy in the calculation of CID requires a model that incorporate inter-turn cross capacitance [5]. Formula for the capacitance between two coaxial cylinders is used in the calculation of CLV.

Inductance

When evaluating the inductance it is assumed that magnetic flux penetration into the laminated iron core is negligible at frequencies above 1 MHz [6]. The inductance can be calculated by assuming the winding consists of loss-less multi-conductor transmission lines surrounded by a homogeneous insulator, hence [4]

$$[L][C] = [C][L] = me\ [I_n] \quad (21)$$

where μ and ε are the permeability and permittivity of the insulation and I_n is the unit matrix. If no high frequency magnetic flux penetrates the iron core, the winding can be regarded as a conductor in free space surrounded by insulation. The inductance due to the flux external to the conductor can be calculated using [7]

$$[L_n] = \frac{e_r}{c^2}[C_n]^{-1} \quad (22)$$

where [C_n] = capacitance without insulation, ε_r = relative permittivity of insulation and c = velocity of light in free space. At high frequencies, the flux internal to the conductor also creates an inductance [4]

$$L_i = \frac{R_S}{2pf} \quad (23)$$

where R_S is the resistance due to the skin effect and f is the frequency. The inductance matrix is given by

$$[L] = [L_n] + L_i[I_n] \quad (24)$$

Resistance

In resistance calculation, the skin effect at high frequencies is taken into account. The resistance per unit length of conductor is given by

$$R_S = \frac{1}{2(d_1 + d_2)}\sqrt{\frac{pfm}{s}} \quad (25)$$

where d_1, d_2 = cross-sectional dimensions of rectangular conductor, μ = permeability of conductor, σ = conductivity and f = frequency.

Conductance

The conductance is due to the capacitive loss in the insulation. It depends upon the frequency f, the capacitance C and the dissipation factor tan δ.

$$[G] = 2\pi f[C]\tan\delta \qquad (26)$$

The tan δ for the Nomex® paper insulation used in this transformer satisfies [8]

$$\tan\delta = 0.07\left(1 - \frac{6}{7}e^{-(0.308\,f\times10^{-6})}\right) \qquad (27)$$

Hence

$$[G] = 0.44\,f[C]\left(1 - \frac{6}{7}e^{-(0.308\,f\times10^{-6})}\right) \qquad (28)$$

SIMULATION RESULTS

The parameters calculated in the previous section are used to determine the transfer functions TF_L and TF_N. The PD current pulses were injected into various turns on the winding. The results are shown in Figure 2 and Figure 3 for f < 2000 kHz.

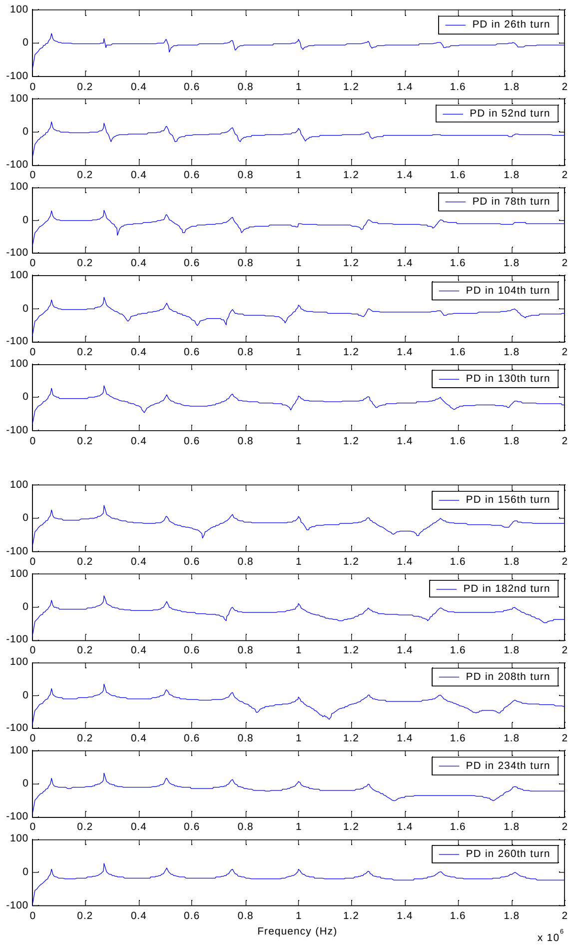

Figure 2 – Magnitude of TF_L (1 kHz ~ 2000 kHz)

Figure 2 shows the transfer functions from the source of the discharge to the line-end (TF_L). PD current pulses were injected at turns 26, 52, 78, 104, 130, 156, 182, 208, 234 and 260 on the winding. Note that these turn numbers are multiples of 26 since each double section has 13×2=26 turns. It is clear from Figure 2 and Table 1 that as the turn number increases the frequency of zeros (minima) increases in value. The frequencies of poles (maxima) are unaffected.

Figure 3 shows the transfer functions from the source of the discharge to the neutral-end (TF_N). The frequency of the zeros decrease in value as turn number increases. As in previous case, frequencies of poles are unaffected. Table 2 gives pole-zero positions.

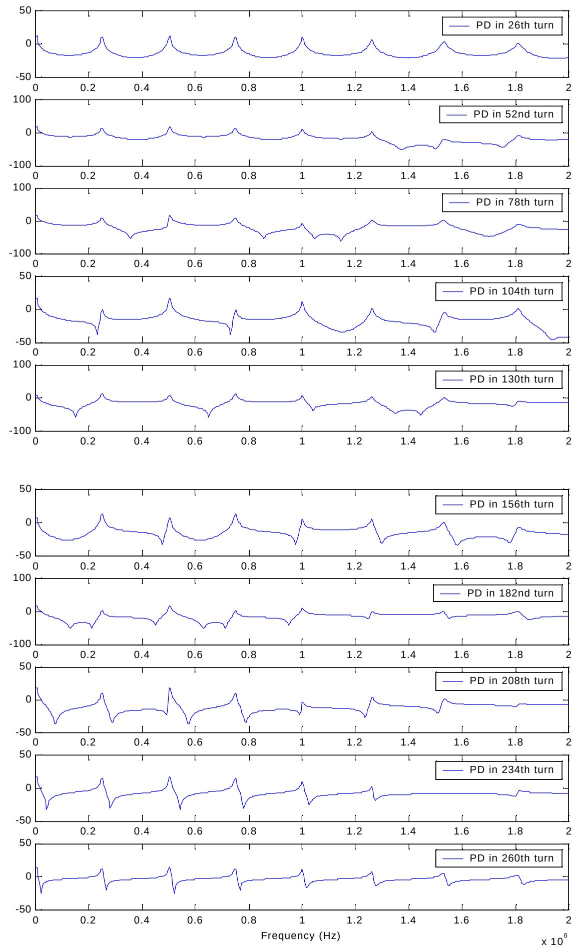

Figure 3 – Magnitude of TF_N (1 kHz ~ 2000 kHz)

CONCLUSION

In a continuous disc type transformer winding, the frequency of zeros in transfer functions from the source of discharge to the line-end and the neutral-end increases in frequency as the discharge source moves away from the measuring terminal and hence verifies previous research on PD location using this approach. The frequency of the first zero is a good indicator of the discharge position along the winding and hence can be used for PD location. The frequency of poles only gives local oscillations for the winding and are unaffected by PD.

Table 1 Pole – zero positions (kHz) of transfer functions TF_L (f =1 kHz ~ 2000 kHz)

PD (turn no.)	p_1	p_2	z_1	p_3	z_2	p_4	z_3	p_5	z_4	P_6	z_5	p_7	z_6	p_8
26	70	271	275	508	520	753	765	1005	1020	1265	1280	1534	1552	1813
52	70	271	295	508	542	753	784	1005	1030	1265	1280	1534	1542	1813
78	70	271	321	508	572	753	792	1005	996	1265	1242	1534	1510	1813
104	70	271	358	508	624	753	730	1005	954	1265	1248	1534	1550	1813
130	70	271	419	508	975	753	1298	1005	1585	1265	1793	1534	-	1813
156	70	271	646	508	1036	753	1355	1005	1454	1265	1790	1534	-	1813
182	70	271	729	508	1488	753	1930	1005	-	1265	-	1534	-	1813
208	70	271	848	508	1120	753	1670	1005	1758	1265	-	1534	-	1813
234	70	271	1360	508	1735	753	-	1005	-	1265	-	1534	-	1813
260	70	271	-	508	-	753	-	1005	-	1265	-	1534	-	1813

Table 2 Pole – zero positions (kHz) of transfer functions TF_N (f =1 kHz ~ 2000 kHz)

PD (turn no.)	p_1	p_2	z_1	p_3	z_2	p_4	z_3	p_5	z_4	P_6	z_5	p_7	z_6	p_8
26	70	271	244	508	-	753	-	1005	-	1265	-	1534	-	1813
52	70	271	172	508	1375	753	1505	1005	1755	1265	-	1534	-	1813
78	70	271	141	508	860	753	1050	1005	1150	1265	-	1534	-	1813
104	70	271	122	508	736	753	1496	1005	1945	1265	-	1534	-	1813
130	70	271	109	508	654	753	1045	1005	1354	1265	1450	1534	1795	1813
156	70	271	99	508	432	753	981	1005	1304	1265	1585	1534	1785	1813
182	70	271	91	508	369	753	634	1005	716	1265	951	1534	1250	1813
208	70	271	84	508	332	753	578	1005	792	1265	991	1534	1240	1813
234	70	271	79	508	306	753	546	1005	786	1265	1030	1534	1280	1813
260	70	271	74	508	287	753	524	1005	768	1265	1020	1534	1282	1813

ACKNOWLEDGEMENT

The first author would like to thank the Open University of Sri Lanka, UMIST, the National Grid Company plc, Alstom (Transmission & Distribution) and the Edison Mission Energy Company for sponsoring this research.

REFERENCES

[1] International Electrotechnical Commission, 'IEC 60270 (2000-12): High voltage test techniques – Partial discharge measurements', 3rd Edition, 2000.

[2] Wang, Z. D., Crossley, P. A., Cornick, K. J., Zhu, D. H., 'An algorithm for partial discharge location in distribution transformers', 2000 IEE/PES Winter Meeting, 23 – 27 January 2000, Singapore.

[3] Cornick, K., Filliat, B., Kieny, C., Muller, W., 'Distribution of very fast transient overvoltages in transformer windings', CIGRE, 30 August – 5 September 1992, Paris, France.

[4] Paul, C. R., 'Analysis of multi-conductor transmission lines', John Wiley & Sons, 1994.

[5] Wang, Z., 'An analytical solution for calculations of inter-disc and inter-winding capacitances in transformer windings' Technical Report (1), UMIST, October 1992.

[6] Guardado, J. L., Venegas, V., Melgoza, E., Naredo, J. L., 'Modelling pulse propagation in high voltage machines', 10th International Symposium on High Voltage Engineering, Montreal, Canada, 25-29 August 1997.

[7] Guardado, J. L., Cornick, K. J., 'A computer model for calculating steep-fronted surge distribution in machine windings', IEEE Transactions on Energy Conversion, Vol. 4, No. 1, March 1989.

[8] Wang, Z., 'Measuring and computing the impedance of a double disc coil', Technical Report (5), UMIST, May 1993.

AUTHOR'S ADDRESS

The first author can be contacted at

Department of Electrical Engineering & Electronics
UMIST
Manchester M60 1QD
UK

Email: s.hettiwatte@student.umist.ac.uk